

# THERMAL PROPERTIES OF CrTaO<sub>4</sub> AND (CrTaTi)O<sub>2</sub>

Morgan Small, Cameron Miller, Dr. Elizabeth Opila  
The University of Virginia

**Abstract** – The purpose of this study is to experimentally determine the coefficients of thermal expansion (CTE) for the complex oxides CrTaO<sub>4</sub> and (CrTaTi)O<sub>2</sub> in order to assess their suitability as protective oxides. Techniques such as Spark Plasma Sintering (SPS), X-ray Diffraction (XRD), Scanning Electron Microscopy (SEM), Energy-Dispersive X-ray Spectroscopy (EDS), and dilatometry were used to prepare, characterize, and test the oxide specimens. A secondary phase of Ta<sub>2</sub>O<sub>5</sub> was found in both oxides by SEM and EDS analysis. The CTEs of CrTaO<sub>4</sub> and CrTaTiO<sub>2</sub> were found to be  $5.9 \times 10^{-6}$  and  $5.6 \times 10^{-6}$ , respectively.

## INTRODUCTION

Due to advancements in aerospace technologies, there is a growing necessity for materials that can withstand extreme environments beyond the capabilities of traditional Ni-base superalloys (e.g., temperatures > 1000°C)<sup>1</sup>. Refractory alloys have gained interest as they have much higher melting temperatures (> 1800°C), retain high-temperature mechanical strength to significantly high temperatures, and avoid complex cooling schemes<sup>1</sup>. However, a challenge of employing refractory alloys is their extremely poor oxidation resistance, which previous research has found to be the main contributor to shorter lifetimes and severe degradation of mechanical properties<sup>2</sup>. The development of refractory complex concentrated alloys (RCCAs) and high entropy alloys (RHEAs) have enabled enhancements in the ability to balance both high-temperature strength and oxidation resistance, albeit for shorter periods of time. RCCAs have been shown to form more complex oxide species due

to the reaction of simple oxides ( $\text{Cr}_2\text{O}_3 + \text{Ta}_2\text{O}_5 \rightarrow 2 \text{CrTaO}_4$ ) that mitigate the presence of deleterious oxides (e.g., Nb<sub>2</sub>O<sub>5</sub>, Ta<sub>2</sub>O<sub>5</sub>), thus providing moderately protective oxidation resistance<sup>1</sup>. Additionally, Schellert et al. elucidated the protective influence of substitution on the cation sublattice in related complex oxides, specifically that substitutional additions of Ti into CrTaO<sub>4</sub> form rutile-structured (Cr,Ta,Ti)O<sub>2</sub><sup>2</sup>. This oxide provides additional beneficial oxidation resistance that is ultimately attributed to the substitution of Ti<sup>4+</sup> on Cr<sup>3+</sup> sites in (Cr,Ta,Ti)O<sub>2</sub>, which is hypothesized to reduce the oxygen vacancy concentration and thus enhance the oxidation resistance.

RCCAs containing Cr, Ta, and Ti are of interest for high-temperature structural applications due to the unique combination of properties they offer. Ta is quite dense (16.65 g/cm<sup>3</sup>) but has a high melting temperature (3017 °C) and offers significant high temperature strengthening potential, but poor oxidation resistance<sup>2</sup>. Cr and Ti have lower densities (7.19 and 4.5 g/cm<sup>3</sup>, respectively) and are known to form favorable oxides with Ta (e.g., CrTaO<sub>4</sub>, (Cr,Ta,Ti)O<sub>2</sub>) as well as classically protective yet volatile Cr<sub>2</sub>O<sub>3</sub>. Four alloys of varying composition in the ternary Ta-Ti-Cr system were recently studied by Welch et al<sup>2</sup>. Equiatomic TaTiCr was found to have the best oxidation resistance, which was attributed to the formation of a dense and compact oxide composed of complex oxides ((CrTaTi)O<sub>2</sub>, CrTaO<sub>4</sub>, and TaTiO<sub>4</sub>) and Cr<sub>2</sub>O<sub>3</sub><sup>2</sup>.

This work reports on experimental efforts to further characterize properties of CrTaO<sub>4</sub> and (CrTaTi)O<sub>2</sub>, specifically their coefficients of thermal expansion.

## EXPERIMENTAL PROCEDURE

### *Coefficient of Thermal Expansion Study Procedure- CrTaO<sub>4</sub>*

A stoichiometric mix of Cr<sub>2</sub>O<sub>3</sub> and Ta<sub>2</sub>O<sub>5</sub> was placed into a cylindrical Nalgene container with zirconia (ZrO<sub>2</sub>) milling media and placed on a ball mill for 24 hours. The blended and refined powder was then inserted into a 1-inch graphite Spark Plasma Sintering (SPS) die. SPS was performed on the sample resulting in a solid puck of CrTaO<sub>4</sub> with density 6.813 g/cm<sup>3</sup>, measured via Archimedes density. Compared to the calculated density of 7.572 g/cm<sup>3</sup> from the Highscore software used for analysis, the sample has a relative density of 91.1 %. Due to the argon environment of the SPS chamber and the graphite die, a reducing environment was created. The puck was annealed in a stagnant air box furnace for 24 hours at 1500 °C to restore oxygen stoichiometry. A slow speed diamond saw was used to cut the puck into two smaller samples, one of which was then tested via X-Ray Diffraction (XRD) to determine crystal structure. This same sample was then prepared for Scanning Electron Microscope (SEM) and Energy Dispersive Spectroscopy (EDS). This sample was polished to 1 μm, sonicated, and sputtercoated with gold and palladium. The specimen was then placed in the SEM to investigate composition and microstructure of the sample. Finally, dilatometry was performed on the second of the two samples to determine CTE. This sample was 14.120 mm by 4.806 mm by 3.734 mm. The peak temperature was set to 1200 °C with heating and cooling rate of 5 °C per minute. After dilatometry, sample density was measured to be 6.900 g/cm<sup>3</sup>. This slight and practically negligible increase in density is most likely due to the compression the sample experienced during dilatometry. Compared to the calculated density of 7.572 g/cm<sup>3</sup> from the Highscore software used for analysis, the sample has a relative density of 90.0%.

### *Coefficient of Thermal Expansion Study Procedure- (CrTaTi)O<sub>2</sub>*

A stoichiometric mix of Cr<sub>2</sub>O<sub>3</sub>, Ta<sub>2</sub>O<sub>5</sub>, and TiO<sub>2</sub> was prepared. The sample preparation methods used follow those already described for CrTaO<sub>4</sub>. Two dilatometry specimens were prepared. Specimen A measured 14.491 mm by 4.456 mm by 4.678 mm and specimen B measured 14.472 mm by 4.145 mm by 4.683 mm. Archimedes density was taken for both specimens, but as specimen A was the only sample used in this study, only the density for specimen A is reported here. The measured density of specimen A is 5.54518 g/cm<sup>3</sup>. Dilatometry and characterization procedures follow those already described for CrTaO<sub>4</sub>.

## RESULTS

### *Coefficient of Thermal Expansion Study- CrTaO<sub>4</sub>*

#### *I. SEM and EDS*

SEM micrographs display the CrTaO<sub>4</sub> oxide puck to be slightly rich in Ta<sub>2</sub>O<sub>5</sub>. Figure 1 provides an overview of the bulk, as captured by the SEM's Everhart-Thornley detector (ETD). The micrograph contains white dispersions throughout the grey CrTaO<sub>4</sub> bulk that were found to be Ta<sub>2</sub>O<sub>5</sub>. EDS area analysis on a dispersion spot confirms the CrTaO<sub>4</sub> puck to be rich in Ta<sub>2</sub>O<sub>5</sub>. The micrograph of a selected dispersion and subsequent EDS analysis are included in Figure 2.

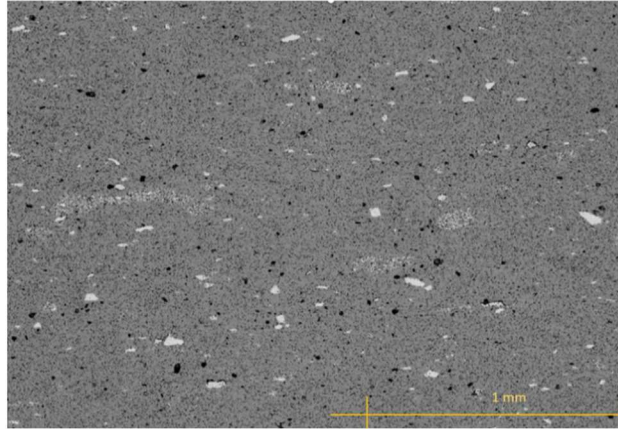


Figure 1: CrTaO<sub>4</sub> Bulk Micrograph

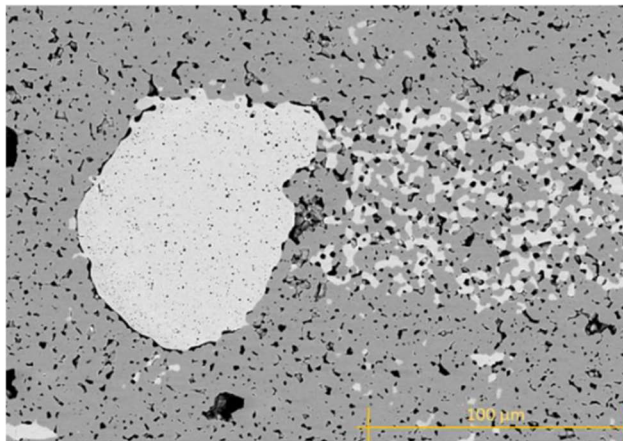


Figure 2: Micrograph and EDS of Ta<sub>2</sub>O<sub>5</sub> dispersion

## II. XRD

Figure 3 shows CrTaO<sub>4</sub> peaks in blue and excess peaks representing Ta<sub>2</sub>O<sub>5</sub> in grey. It is worthy to note that there was a direct reference card in the Highscore software used to process

this XRD data, which was provided by Krylov E.I et. al.<sup>4</sup>. Figure 4 shows an XRD spectrum of the rutile structure, which is consistent with the peak pattern shown in Figure 3<sup>5</sup>.

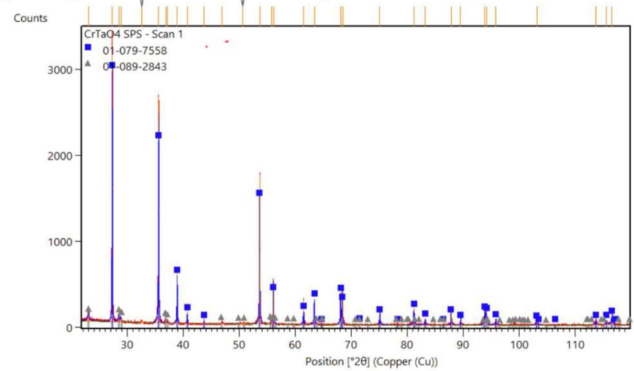


Figure 3: XRD spectra for CrTaO<sub>4</sub>

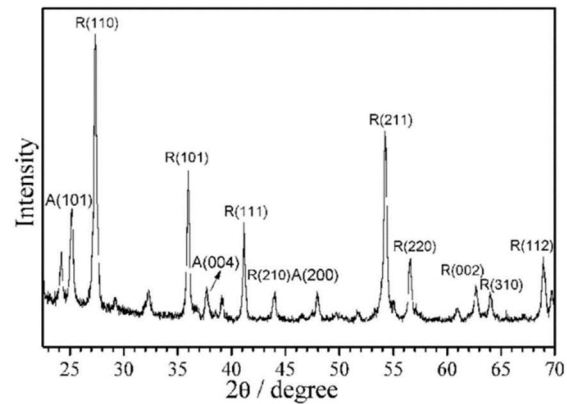


Figure 4: Common XRD pattern of a rutile structure

## III. Dilatometry

The linear CTE of CrTaO<sub>4</sub> was found to be  $5.9 \times 10^{-6}/^{\circ}\text{C}$  by dilatometry as shown in Figure 5. This result is consistent with coefficients of other rutile oxides, which are typically on the order of  $10^{-6}/^{\circ}\text{C}$ .

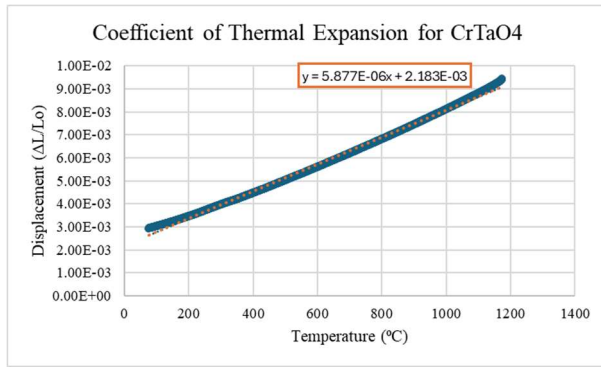


Figure 5: Dilatometry heating curve for CrTaO<sub>4</sub> with linear regression equation result

### *Coefficient of Thermal Expansion Study-(CrTaTi)O<sub>2</sub>*

#### *I. SEM and EDS*

Figure 6 provides a compositional bulk micrograph of (CrTaTi)O<sub>2</sub>. Similarly to CrTaO<sub>4</sub>, the micrograph contains white dispersions of excess Ta<sub>2</sub>O<sub>5</sub> throughout the (CrTaTi)O<sub>2</sub> bulk, but at a higher phase fraction. This is confirmed by EDS analysis of a smaller area of interest. The area of interest is shown in Figure 7 as captured by the ETD detector. A backscatter (BSE) image of this area is provided in Figure 8 for clarity. The EDS for this area of interest and the resulting EDS maps are provided in Figures 9 and 10. It is clear that the large white dispersions are a secondary phase of Ta<sub>2</sub>O<sub>5</sub>.

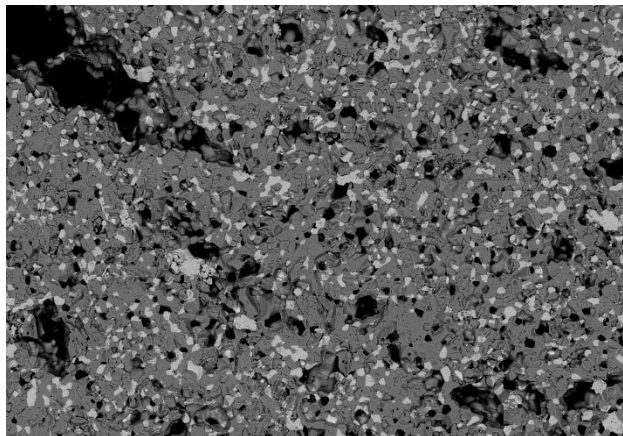


Figure 6: Compositional bulk micrograph of CrTaTiO<sub>2</sub>

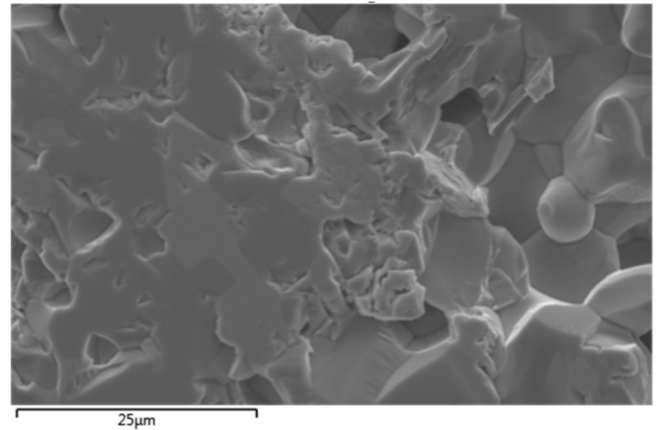


Figure 7: Micrograph of area of interest within (CrTaTi)O<sub>2</sub> puck

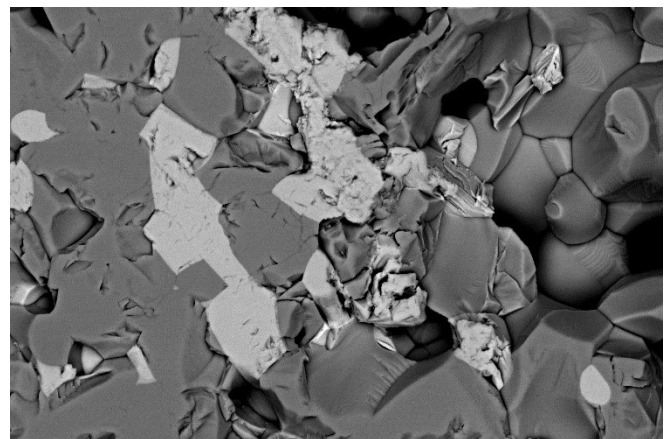


Figure 8: Compositional micrograph of area of interest within (CrTaTi)O<sub>2</sub> puck



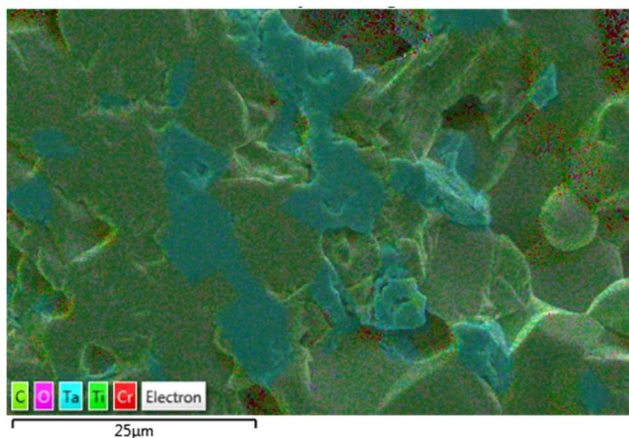


Figure 9: Layered EDS map of area of interest within (CrTaTi)O<sub>2</sub> puck

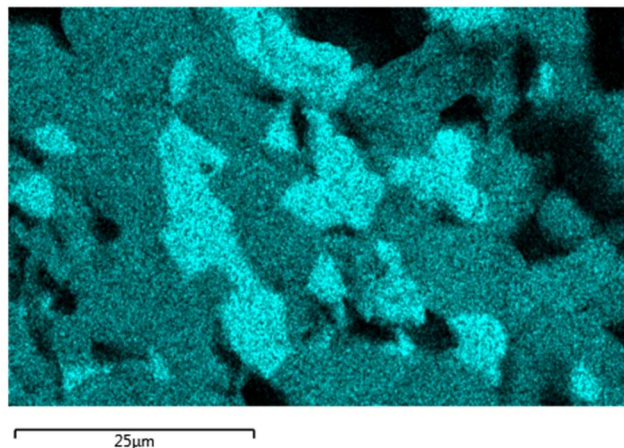


Figure 10: EDS map of Ta<sub>2</sub>O<sub>5</sub> present in area of interest

In order to further investigate the composition of these inclusions, EDS point scans were conducted. Figure 11 displays the results of an EDS point scan done on the grey sample bulk. It shows a relatively even composition of Cr, Ta, and Ti as expected. This indicates the successful synthesis of (CrTaTi)O<sub>2</sub>. Any trace amounts of gold (Au) or palladium (Pd) found via EDS are attributed to the sample coating required for SEM of nonconductive samples.

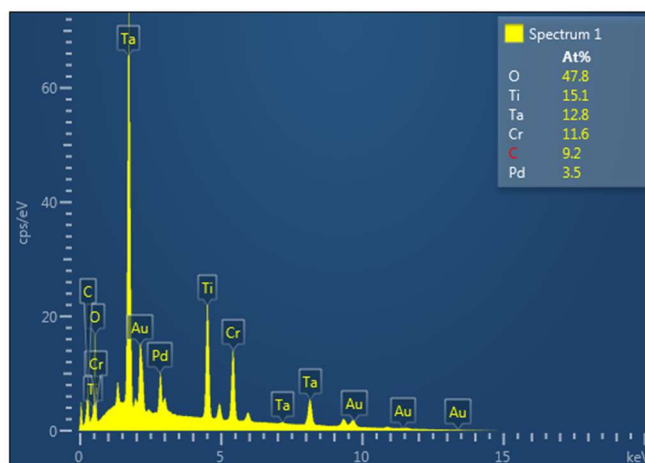


Figure 11: EDS point scan of grey specimen bulk

An EDS point scan was also conducted on one of the white phases. The spot was found to be consistent with Ta<sub>2</sub>O<sub>5</sub> with almost no Cr or Ti present. These results are provided in Figure 12. It is clear that Ta<sub>2</sub>O<sub>5</sub> is a secondary phase of this (CrTaTi)O<sub>2</sub> puck under the selected processing conditions.

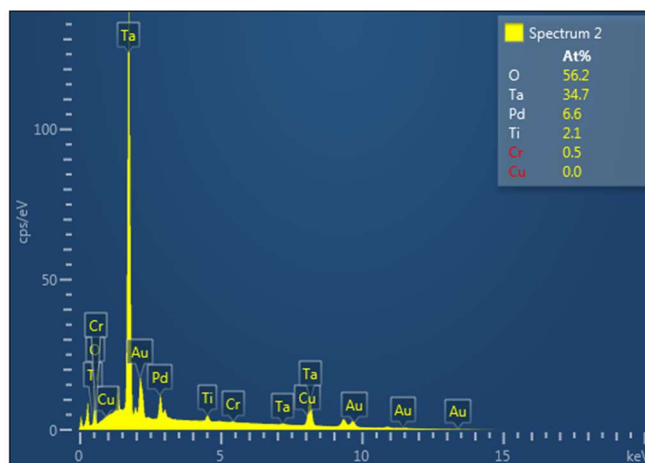


Figure 12: EDS point scan of white Ta<sub>2</sub>O<sub>5</sub> dispersion

## II. XRD

It is important to note that results reported in this section are the product of a different (CrTaTi)O<sub>2</sub> synthesis made prior to the

creation of the oxide puck used for the previous section.

Figure 13 displays  $(\text{CrTaTi})\text{O}_2$  peaks in blue and excess peaks representing  $\text{Ta}_2\text{O}_5$  in green. It is worthy to note that there was a direct reference card in the Highscore software used to process this XRD data, which was provided by Mani et. al <sup>5</sup>. This pattern is once again consistent with a rutile structure, as provided in Figure 4. Thus, it is reasonable to assume that linear CTE of  $(\text{CrTaTi})\text{O}_2$  will also be on the order of  $10^{-6}$ .

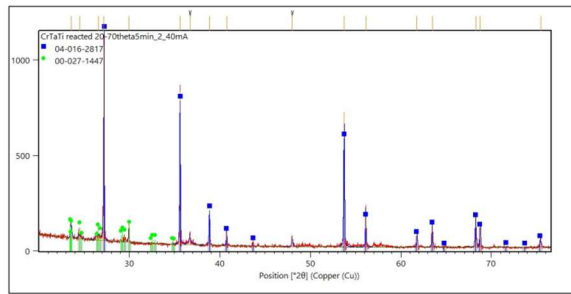


Figure 13: XRD spectra for  $(\text{CrTaTi})\text{O}_2$

### III. Dilatometry

The linear CTE of  $(\text{CrTaTi})\text{O}_2$  was found to be  $5.6 \times 10^{-6}/^\circ\text{C}$  by dilatometry as displayed in Figure 14. This result is consistent with coefficients of other rutile oxides, which are typically on the order of  $10^{-6}$ .

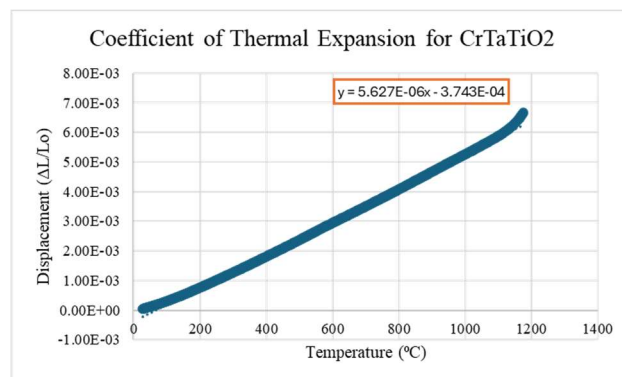


Figure 14: Dilatometry heating curve for  $(\text{CrTaTi})\text{O}_2$  with linear regression equation result

## DISCUSSION

### SEM and EDS

#### I. $\text{CrTaO}_4$

The excess  $\text{Ta}_2\text{O}_5$  present in the  $\text{CrTaO}_4$  puck could be a result of: volatilization of  $\text{Cr}_2\text{O}_3$  during oxide formation, a measurement error when creating the powder mixture, a processing issue, or an unknown catalyst for secondary phase formation. Future work will investigate the phase fraction of  $\text{CrTaO}_4$  to excess  $\text{Ta}_2\text{O}_5$ .

#### II. $(\text{CrTaTi})\text{O}_2$

The SEM images collected of  $(\text{CrTaTi})\text{O}_2$  very clearly show a multi-phase structure. This is consistent with the XRD spectra in Figure 13.

### XRD

#### $\text{CrTaO}_4$ and $(\text{CrTaTi})\text{O}_2$

The XRD spectra in Figures 3 and 13 confirm the successful synthesis of rutile oxides  $\text{CrTaO}_4$  and  $(\text{CrTaTi})\text{O}_2$ . The spectra show an excess of  $\text{Ta}_2\text{O}_5$ , which is consistent with the  $\text{Ta}_2\text{O}_5$  dispersions present in the SEM micrographs.

### Dilatometry

CTEs of  $\text{CrTaO}_4$  and  $(\text{CrTaTi})\text{O}_2$  were found to be  $5.9 \times 10^{-6}/^\circ\text{C}$  and  $5.6 \times 10^{-6}/^\circ\text{C}$ , respectively. This is a reasonable result as compared to other oxides of a rutile structure, such as the oxide  $\text{TiO}_2$  which has a CTE range of  $(8.4-11.8) \times 10^{-6}/^\circ\text{C}$ .

The effect the secondary phase of  $\text{Ta}_2\text{O}_5$  has on the CTE of  $(\text{CrTaTi})\text{O}_2$  is currently unknown. The CTE of  $\text{Ta}_2\text{O}_5$  was found to be  $3.786 \times 10^{-6}/^\circ\text{C}$ .

$10^{-6}/^{\circ}\text{C}$  by Brown et. al. which is considerably smaller than the experimental CTE of  $(\text{CrTaTi})\text{O}_2$ <sup>6</sup>. The difference in CTEs could cause internal stresses or uneven expansion. It is worthy to note that secondary phase formation may be due to processing conditions such as the synthesis temperature used during SPS, thus future investigations will involve varying processing conditions.

### CONCLUSION

The CTEs of  $\text{CrTaO}_4$  and  $(\text{CrTaTi})\text{O}_2$  were found by dilatometry to be  $5.9 \times 10^{-6}/^{\circ}\text{C}$  and  $5.6 \times 10^{-6}/^{\circ}\text{C}$ , respectively. SEM and EDS characterization helped to identify the presence of a secondary phase of  $\text{Ta}_2\text{O}_5$  in each oxide. XRD results confirmed the successful synthesis of both oxides as well as the presence of excess  $\text{Ta}_2\text{O}_5$ . The cause of the secondary phase formation is unknown, but will be investigated in future work.

### CONCURRENT STUDY AND FUTURE WORK

A concurrent study is being conducted by Hunter Schonfeld and Patrick Hopkins at the University of Virginia to determine the melting temperatures of  $\text{CrTaO}_4$  and  $(\text{CrTaTi})\text{O}_2$ . Preliminary results show the melting temperatures of both oxides to be approximately  $2100^{\circ}\text{C}$ .

Future work related to this research includes the use of ImageJ to determine the area fraction of the secondary  $\text{Ta}_2\text{O}_5$  phase in micrographs of  $\text{CrTaO}_4$  and  $(\text{CrTaTi})\text{O}_2$ . It is also intended to use hot stage XRD to authenticate the CTEs determined by dilatometry. Additionally, studies to determine the effects of the secondary  $\text{Ta}_2\text{O}_5$  phase on CTE will be conducted. Oxygen diffusivity will be determined once pure phases are synthesized.

### ACKNOWLEDGMENTS

I would like to acknowledge Dr. Elizabeth Opila for her constant support and guidance

throughout this project. I would also like to acknowledge the training and support I received from Cameron Miller and Clark Luckhardt that made this research possible. Hunter Schonfeld's contributions to a melting temperature study for these oxides cannot be overstated, and will be included in a future publication.

### REFERENCES

1. Noah J. Welch, Maria J. Quintana, Samuel J. Kuhr, Todd M. Butler, Peter C. Collins, Intermediate and high-temperature oxidation behavior of an equiatomic TaTiCr RCCA from  $800^{\circ}\text{C}$  to  $1400^{\circ}\text{C}$ , International Journal of Refractory Metals and Hard Materials, Volume 118, 2024, 106437, ISSN 0263-4368, <https://doi.org/10.1016/j.ijrmhm.2023.106437>. (<https://www.sciencedirect.com/science/article/pii/S0263436823003372>)
2. S. Schellert, M. Weber, H.J. Christ, C. Wiktor, B. Butz, M.C. Galetz, S. Laube, A. Kauffmann, M. Heilmaier, B. Gorr, Formation of rutile  $(\text{Cr,Ta,Ti})\text{O}_2$  oxides during oxidation of refractory high entropy alloys in Ta-Mo-Cr-Ti-Al system, Corrosion Science, Volume 211, 2023, 110885, ISSN 0010-938X, <https://doi.org/10.1016/j.corsci.2022.110885>. (<https://www.sciencedirect.com/science/article/pii/S0010938X22008034>)
3. Du, Jianzhong & Sun, Hui. (2014). Polymer/ $\text{TiO}_2$  Hybrid Vesicles for Excellent UV Screening and Effective Encapsulation of Antioxidant Agents. ACS applied materials & interfaces. 6. 10.1021/am502663j.
4. Krylov E.I., Rozhdestvenskii F.A., Potekhin O.G., Solomennikov V.K., Inorg. Mater. (Engl. Transl.), 4, 410, (1968)

5. Mani R., Achary S.N., Chakraborty K.R., Deshpande S.K., Joy J.E., Nag A., Gopalakrishnan J., Tyagi A.K., Adv. Mater. (Weinheim, Germany), 20, 1348-1352, (2008)

6. Brown Jr, Jesse Jefferson. "Solid State Reactions and Thermal Expansion of Phases in Systems Containing Zinc-Oxide and Selected Oxides of the Groups IV and V Elements." PhD diss., The Pennsylvania State University, 1964.

#### **AUTHOR INFORMATION**

Morgan Small. Undergraduate Student at the University of Virginia, Department of Materials Science and Engineering. Materials Research Engineer for Analytical Services and Materials (AS&M), NASA Langley Research Center.